# Effects of SiC On the Microstructure, Densification, Hardness and Wear Performance of $TiB_2$ Ceramic Matrix Composite Consolidated Via Spark Plasma Sintering

**Samson Dare Oguntuyi** ( samsoniumdare@gmail.com )
Tshwane University of Technology Pretoria Campus https://orcid.org/0000-0001-8691-8776
**Mxolisi Brendon Shongwe**
Tshwane University of Technology
**Lerato Tshabalala**
Council for Scientific and Industrial Research
**Oluwagbenga T. Johnson**
Department of Mining and Metallurgical Engineering, University of Namibia
**Nicholus Malatji**
Tshwane University of Technology

**Research Article**

**Keywords:** Microstructure, Densification, Hardness, Wear Performance, TiB2, SiC

**Posted Date:** October 5th, 2021

**DOI:** https://doi.org/10.21203/rs.3.rs-884916/v1

# Abstract

Monolithic $TiB_2$ are known to have a good combination of densification and hardness which are sometimes useful but limited in application. However, their usage in service at elevated temperatures such as in power thermal plants, cutting tools, tribological purposes (cutting tools, mechanical seals, blast nozzles, and wheel dressing tools), etc leads to catastrophic failure. Hence, the introduction of sintering additives in the $TiB_2$ matrix has a high influence on the improvement of its sinterability, and properties (fracture toughness, wear resistance etc.,) of the resulting composite needed to meets the requirement for various industrial applications. In this study, the influence of SiC as sintering additives on the microstructure, densification, hardness and wear performance of $TiB_2$ ceramic was observed. Hence, $TiB_2$, $TiB_2$-10wt%SiC and $TiB_2$-20wt%SiC were sintered at 1850 $^oC$ for 10 minutes under 50 MPa. The impacts of SiC on the $TiB_2$ were observed to improve the microstructure correspondingly improving densification and mechanical properties, most especially with the composites with 20wt% SiC. Combined excellent densification, hardness and fracture toughness of 99.5%, 25.5 GPa, 4.5 $MPa.m^{1/2}$ were achieved respectively for $TiB_2$-20wt%SiC. Diverse in-situ phase and microstructural alterations were detected in the sintered composites, and it was discovered that the in-situ phase of TiC serves as the contributing factor to the enhanced features of the composites. Moreover, the coefficient of friction and wear performance outcomes of the synthesized composites described a decrease in the coefficient with an enhanced wear resistance via the increasing SiC particulate, although the application of the load from 10 N-20 N increased the wear rates.


# 1. Introduction

Titanium diboride ($TiB_2$) is among the family of transition metal compounds that are regarded as ultrahigh temperature ceramics [1]. $TiB_2$ ceramic matrix possesses some excellent properties such as chemical stability in harsh environments, high melting points, good thermal conductivity, good abrasion resistance high strength, and hardness [2–4]. These properties have made it possible for $TiB_2$ to be used in various applications viz aluminium evaporator boats, cutting tools, ballistic armour, wear-resistant parts, etc [5, 6]. Despite the excellent performance of these materials in service, their poor self-diffusion coefficient, high melting point, the existence of oxide contaminants ($B_2O_3$ and $TiO_2$) on the powder surface of $TiB_2$ and strong covalent bonding pose some challenges in densification of monolithic $TiB_2$ [6, 7]. Previous works have stated that in achieving a theoretical density of more than 98% of a monolithic $TiB_2$, an elevated consolidation temperature with high external pressure is required. However, grain growth developed at these high consolidation temperatures often reduces the flexural strength and fracture toughness as well as some of its intrinsic properties [8, 9]. Thus, numerous works have been done to enhance the mechanical properties and the sinterability of $TiB_2$ ceramics materials via the introduction of non-metallic additives and metallic as sintering aids. Metallic additives such as Fe, Al, Ti, Cr, Ta etc, are applied for $TiB_2$ ceramic densification but their usage has been limited as a result of their depreciating effects on the high-temperature application of $TiB_2$. Owning to these challenges, attention has been

shifted to densifying $TiB_2$ with the use of non-metallic additives which are mostly carbides, silicides, nitrides and borides-based sintering aid such as, AlN, TiC, WC, $Si_3N_4$, NbC, SiC, $ZrB_2$ [10–14]. These additives remove oxide layers from the powder surface or create in-situ phases which contribute to the composites' sinterability and properties enhancement [11, 15, 16].

Spark plasma sintering is the one of the fabrication processes that is used for the consolidation of $TiB_2$ ceramic materials. This technique uses a lower temperature to achieve the densification of ceramics material under low pressure at a short dwell time, these have made SPS gain high predominance over other conventional sintering viz, hot press, hot isostatic press, etc. The application of SPS ensures the achievement of high densification, finer microstructure and excellent mechanical properties [17–19].

In addition, the importance of fine microstructure, peak densification and excellent mechanical properties cannot be jettisoned in the enhancement of wear performance. Hence in the achievement of these features, judicious selection of the type of sintering additives/matrix and their right composition has a lot of priority. The utilization of ceramic matrix composites for cutting tools and other applications where wear behavior is highly considered, certain things must be measured so as to design the type of materials that can withstand the wear rate, thus the type of load, time and the type of medium the material will be used will be put into consideration. It has been studied that under dry sliding parameters that the tribological performance of ceramic components is difficult and reliant on some outward conditions such as sliding speed, humidity, temperature, load counterpart atmosphere, etc [20].

Past works have emphasized the influence of carbides and nitrides reinforcement on the relative density and mechanical features of borides ceramic. The inclusion of 5 wt% silicon nitride ($Si_3N_4$) in $TiB_2$ ceramic matrix as a sintering aid was observed. It was reported that there was a densification increment when it was sintered via SPS at the temperature of 1900°C under 40 MPa for 7 min. [4]. It was reported that the incorporation of 2.5 wt% $Si_3N_4$ to $TiB_2$ matrix enhances the sinterability of the composites significantly when it was hot-pressed at 1800°C for 1 h [6]. The examination of the impact of diverse composition of SiC particulates under varying sintering parameters were studied on the consolidation of $TiB_2$ based composites. A densification of 99.5% was attained at the temperature of 1800 ℃ under 30 MPa for 15 min. Although, at 1600–1800 ℃, under 10–30 MPa for 5–15 min the composites were consolidated [7]. At the grain interface of the reinforcement (SiC) and the matrix ($TiB_2$), the secondary interfacial phase (TiC) which was created via the reaction between the surface oxide contaminants and the SiC particles was reported to improve the densification [10, 21, 22].. An examination was carried-out on the influence of TiN and SiC as an additive and reinforcement on $TiB_2$ based composites synthesized via SPS at 1900°C for 7 min under 40 MPa. A densification of 99.9 % was achieved for the composites of $TiB_2$–SiC (20 vol%)-TiN (5 wt%) and $TiB_2$-SiC (20 vol%) [23] in contrast to the undoped $TiB_2$ under similar sintering parameter which has its densification equal to 96.7% [4].

The inclusion of TiN and SiC was reported to form an in-situ phases, which concurrently improve the densification and sinterability of the two samples [4, 24, 25]. Finer microstructure was examined to be

produced because of the addition of TiN, this experimental work also concur with Shayesteh et al [26], when he only used TiN as a dopant for $TiB_2$. Alexander et al. [27] studied the wear performance of $B_4C$-carbon nanotube and achieved a specific wear rate of 1.06 X $10^{-6}$ $mm^3$/N.m which was less than the undoped $B_4C$ ceramics. Murthy et al. examined that the addition of $ZrO_2$ to $B_4C$ ceramic matrix, created in-situ $ZrB_2$ and consequently round pores of sub-micron size were similarly formed. Hence, the establishment of CO gas could aid to arrest and/or deflect cracks, thus enhancing the tribological behavior of $B_4C$ ceramics. Sharma et al. [28] stated that with a rise in load, the specific wear rate of SiC decline and then the coefficient of friction initially increase and then decline. Sonber et al [29] discovered that the specific wear rate of $B_4C$ enhances with a rise in load, consequently, its coefficient of friction declined.

Profound works have been carried out on the microstructure, densification and mechanical properties of $TiB_2$ using SiC as a sintering additive, but little or no work has been reported on the influence of microstructures and mechanical properties of this composite on it wear performance. Therefore, in this study, the impacts of SiC on the microstructure, relative density, and mechanical properties and the wear performance of $TiB_2$ ceramic were observed, and more importantly, the influence of these aforementioned properties was study on the wear behavior of $TiB_2$-SiC.

# 2. Experimental Procedure

# 2.1 Materials and Process

### (a) Powders and Sample Preparation

The starting available powder $TiB_2$ (purity: 99.5%) produced by H.C. Starck Berlin Werk Goslar, SiC powder (purity: 99.5%), produced by USA (F.J. Brodmann & Co.) were applied

As it is stated in Table 1. The initial powder such as Titanium diboride was used as a matrix, silicon carbide was used as a reinforcement in the matrix ceramics, following the specification as designated by the suppliers. The powders were prepared into two varying compositions of powder viz, $TiB_2$-10wt%SiC and $TiB_2$-20wt%SiC. The XRD of the as-received powders and the mixed compositions are shown in Fig. 2 and Fig. 4. The compositions were mixed in a turbula mixer ((WAB TURBULA SYSTEM SCHATZ)) at a revolution of 78 rpm for 6 h.

The compositions $TiB_2$-10wt%SiC and $TiB_2$-20wt%SiC were discharged in a graphite die (having an inner diameter of 20 mm), a graphite foil is placed in between the powder and the walls of the die and also between the punch and the powder. The graphite foil was used to prevent friction between the die and the powder during the consolidation process and also for easy removal of the as-sintered compact after the consolidation process. The sinter chamber was kept under a vacuum of ($10^{-2}$ Pa) during the experiments. Via the pyrometer which is attached to the grafoil die, the sintering temperature was

observed, controlled and measured. The heating rate of 150 $^{o}$C/min was induced by an alternating current along with a frequency of 50 Hz, this was done until the sintering temperature was raised to the specified temperature (1850 $^{o}$C). A pressure and dwell time of 50 MPa and 10 min were employed during the sintering cycle. Before the removal of the sintered compacts from the sintering chamber, they were allowed to cool at normal temperature. The cooled samples were sandblasted to eliminate any contaminants of the graphite (placed between the surface of the powder and the die) on the surface of the sintered samples.

### (b) Characterization of the sintered samples

The relative density of the as-sintered compacts was calculated via a densitometer which is established on Archimedes principle. For the metallographic analysis, metallographic techniques were used to prepare the transverse cuts of the sintered samples. The compacted sintered samples were ground by abrasives emery papers of different grit sizes 320, 400, 600, 800, 1200, 1400, and polished with diamond suspensions (sizes 1, 3 and 6 μm ), with Kroll's reagent (2 ml HF, 92 ml $H_2O$, and 6 ml $HNO_3$). The elemental, topography and microstructure of the sintered compacts were observed and analyzed via 7600F Field-Emission Scanning Electron Microscope (FESEM, JEOL 7600F) with Energy Dispersive X-ray Spectroscopy (EDS). The X-ray diffractometer (XRD, PW1710 Philips) was used for phase identification.

The Micro-hardness tester (FM-700 FUTURE-TECH) was used to determine the Vickers microhardness. A force of 2 Kg with a dwell time of 15 s. For each sample, 10 measurements were carried out and the mean value of the results was obtained in (GPa) value for the sintered sample. The fracture toughness was estimated via the crack length measurement created by the indenter as revealed in Fig. 1, at a load of 2kg, the measurement (crack length) was done with an optical microscope. Then the formula suggested by Fukuhara et al [30–32] equ. 1, was used to estimate the fracture toughness of the sample

$$K_{ic}=0.203Hv\ a^{1/2}(c/a)^{-3/2} \quad \ldots\ldots (1)$$

Where, Hv – Vickers hardness

2a – diagonal of the indenter

2c – total indentation crack length.

At least 5 indentation examination and their mean value of the data were reported

### (c) The examination of Dry sliding wear

The tribology test was done with (MFT-5000), RTec universal tribometer beside with reciprocating wear drive to contrast diverse loads because loads govern a fundamental role in wear features of components. An exact linear platform was engaged to grip the sample which was attached to a rod and then put into motion. The motion was engaged via the exterior motor that was attached to the functioning stage. Different loads of 5 N, 10 N, 15 N and 20 N using stainless steel ball of diameter 6 mm were engaged at a

linear speed of 0.06cm/s for 900 seconds. The wear test was done on a square sample of size (10 x 10 mm) after its surfaces have been grounded and polished so that SEM can be used to characterize and capture the wear tracks and thus the worn-out surfaces can be seen clearly.

Table 1,
The description of the as-received powder

| Materials | Particle shape | Density | Particle size | Purity (%) | Supplier |
|---|---|---|---|---|---|
| $TiB_2$ | Irregular | 4.52 | 5,1 micron | 99.5 | H.C. Starck Berlin Werk Goslar |
| SiC | Irregular | 3.21 | -325 Mesh | 99.5 | USA (F.J. Brodmann & Co.) |

# 3. Results And Discussions

# 3.1 The Characterization of Feedstock Powder and mixed powder

The features of the as-received $TiB_2$ matrix and sintering additive of SiC are shown in Figs. 2 and 3 and their elemental compositions are shown and analyzed via EDX (Fig. 3). Furthermore, the XRD observation detected that the peaks are mostly of $TiB_2$, and SiC, however, there are discoveries of some oxide contaminants as revealed by the XRD and EDX analysis. $B_2O_3$ and $TiO_2$ are seen on $TiB_2$ surface while $SiO_2$ is detected on the SiC surface. These types of contaminants can be associated with the covering oxide layers which are created on the surface of non-oxide ceramics. The mixed composites ($TiB_2$-10SiC and $TiB_2$-20SiC) examined via the XRD and SEM depicted that there is an obtainment of uniform distribution of the powder matrix and the reinforcement The XRD patterns and the SEM images of the as-mixed composite powders are revealed in Fig. 4 and Fig. 5 respectively.

# 3.2 Relative Density

Figure 6, revealed the densification of the as-sintered composites, which was observed to increase as the SiC increases from 10–20% in the composites. The percentage increase of the composite $TiB_2$-10 SiC and $TiB_2$-20 SiC in contrast to the undoped $TiB_2$ are 1.12% and 3.6%. The development performance of the doped sample is being credited to the emergence of in-situ phases such as TiC, which properties will be later discussed. Figure 6 gives the correlation between the undoped $TiB_2$ and the doped $TiB_2$ with SiC. The graph depicts that with increasing SiC composition, the composite of $TiB_2$-10 SiC and $TiB_2$-20 SiC have their relative density equivalent to 96.99 % and 99.50% respectively in contrast to the undoped $TiB_2$ with densification equal to 95.9%. This outcome infers that the fraction percentage of SiC improves the relative density and sinterability of $TiB_2$. In addition, the sintering parameter of 1850 $^oC$/50 MPa/10 min was observed to be of high influence for the composites, as it minimizes the establishment of pores on the surface of the sintered composites.

# 3.3 Microstructural Evaluation of Sintered sample

Figure 9(b and c) depicted that the grains of the as-sintered composites are wholly connected signifying an excellent sinterability between the matrix and the reinforcement depicted. Although, the existence of several in-situ interfacial phases is greater in the sample with a higher percentage of reinforcement ($TiB_2$-20SiC) than the sample with less reinforcement ($TiB_2$-20SiC. No notable grain growth was detected during the SPS. The introduction of SiC was observed to inhibit grain growth in $TiB_2$ based ceramics. Thus, the attained fine-grained microstructure of the doped $TiB_2$ was not only credited to the existence of SiC as well as some various formed in-situ secondary phases especially TiC but also the relatively short dwell time and the lower sintering temperature of the SPS which contributed to the reduced grain growth. The effective impact of SiC has similarly been examined in the consolidation of $ZrB_2$ based composites, SiC with the use of lower sintering temperature was detected to minimize grain growth [33–35]. XRD sprectra depicted in Fig. 7 confirmed the presence of secondary or in-situ phases in $TiB_2$-10SiC and $TiB_2$-20SiC composites. A synonymous work carried out by Ahmadi et al [24], stated that on the surface of the starting powder of $TiB_2$ there was a development of $B_2O_3$ and $TiO_2$ oxide layer. Although the oxygen content was observed to decline, this was due to the sintering manner caused by the chemical reactions. The achievement of the reaction between the oxide layer of SiC and $TiO_2$ produced some products of $SiO_2$ and TiC, this was examined by HSC chemical software (Equ. 2). The Gibb's free energy for this reaction is -80 kJ, signifying a thermodynamic approval. The creation of in-situ phases of TiC and $SiO_2$ vindicated the validity of the reaction as depicted via the XRD patterns (Fig. 7).

$SiC + TiO_2 - SiO_2 + TiC$…… (2)

Moreover, the development of $SiO_2$ attained during the consolidation procedure can promote the relative density enhancement in the sintered compact composite via the liquid phase sintering mechanism. The sintering temperatures for melting and boiling of $B_2O_3$ oxide layer are at 450 $^oC$ and 1860 $^oC$ in the atmospheric condition of 1atm, respectively. The evaporation of $B_2O_3$ occurs at a temperature less than 1600 $^oC$, this achievement is credited to the stages of vacuum of the sintering atmosphere. Finally, the oxide layer of $B_2O_3$ combines with SiC, established on Equ. 3, generating $B_4C$ and various byproducts in the gaseous phase. Thermodynamically, Equ. 3 is attainable at temperatures of 1750 $^oC$ [36].

$4B_2O_3 + 7SiC - 2B_4C + 7SiO + 5CO$ …….. (3)

For clarity purpose, the elemental composition of the sintered composite ($TiB_2$-20SiC) is analyzed in the EDX (Fig. 8). Based on this EDX outcome, the gray and bright phases were identified to be SiC additive/reinforcement and ceramic matrix, respectively. The black phases are either pores or the grain pull-out during polishing. Similar results were obtained when the samples were characterized using an optical microscope (OPM) as shown in Fig. 10. The presence of pores in ceramic materials can reduce their density. Therefore the measured relative density is consistent with the fractured surface images (Fig. 11), and this backed the outcomes that the porosity of $TiB_2$-20SiC < $TiB_2$-10SiC < $TiB_2$. The attainment of lower relative density in $TiB_2$ in respect to the higher densification of $TiB_2$-10SiC and $TiB_2$-20SiC was

ascribed to the surface pits and pores which could be as a result of grains pullout of the reinforcement or the matrix during the polishing (Fig. 9) [37]. It has been stated that the existence of oxide contaminants on the diborides surface (e.g $HfB_2$, $TiB_2$, and $ZrB_2$) not only initiates grain growth but also lowers the densification process. Thus, the introduction of the sintering additive (SiC) was observed to be beneficial in eliminating the oxide contaminants from the surface of the sintered $TiB_2$ and which consequently promote some in-situ phases which contributed to the enhancement of the composites densification [21, 38]..

# 3.4 Mechanical Properties

In regards to the experimental outcomes, it is revealed that the hardness of the sintered composites got to its peak when the 20 % reinforcement (SiC) was introduced into the matrix. Hence $TiB_2$-20SiC has a hardness of 25.5 GPa, which is 29.01 % greater than the monolithic $TiB_2$ (18.1 GPa). Then the composite having 10% reinforcement of SiC ($TiB_2$-10SiC) has a hardness of 19.05 GPa, which is a 5% increment when compared to monolithic $TiB_2$ (Fig. 12). For the fracture toughness, there was a huge improvement in the fracture toughness of the reinforced composites ($TiB_2$-SiC) in comparison with $TiB_2$, which was credited to the second phase of SiC. The lower outcome of the monolithic $TiB_2$ sample (3.30 $MPa.m^{1/2}$) as shown in Fig. 12, was majorly due to its lower densification (95.9 %) and this fracture toughness improve to 3.8 $MPa.m^{1/2}$- 4.5 $MPa.m^{1/2}$ with increasing additive of SiC.

Microstructural features viz, second phases, porosity, and grain size have huge impacts on mechanical properties. Furthermore, hardness and fracture toughness of ceramics are mostly affected by their relative density [39]. This observation were demonstrated by the experiment carried out by Ghafuri et al [37]. They reported that the enhanced fracture toughness and micro-hardness are credited to the reduced porosity and increased densification [3, 40]. Usually, the fracture toughness of ceramics is not only subjected to its relative density but also its grain size. The larger size of grain particles tends to lower their fracture toughness, which inhibits the improvement in the overall mechanical properties. Although a reduced grain size promotes more cracks deflections and grain boundaries, all these caused crack propagation which allows the consumption of fracture energy. Therefore, reducing grain size increases the fracture toughness of composites [41]. Balak et al [42], recommended that a dwell time of 8 min and a peak temperature of 1700$^oC$ can be used to achieve the sintering of $ZrB_2$-SiC based composites with enhanced properties. They further stated that the composites' fracture toughness would depreciate if the sintering conditions are increased. They upheld that increased grains would be connected with low strength so as to restrict crack propagation. Though higher dwell times and temperatures tend to induce open pores and these consequently cause a reduction in fracture toughness due to grain coarsening. Hence, fracture toughness improvement is majorly controlled by grain size rather than open porosity. Crack deflection around the boundaries of the $TiB_2$/SiC and the SiC particles influenced a major role in the toughening mechanism of the sintered materials. The thermal residual stress which is initiated by the lack of congruence between the coefficient of heat expansion of the SiC grains and $TiB_2$ was observed to promote the crack-microstructure connections [39]. The compressive stresses in the particulates phase of

SiC caused a crack deflection which consequently promotes a huge stress relaxation at the crack tip to decline the dynamic force for crack movement and hence, the toughness of the samples is enhanced.

In addition to the fracture toughness, crack bridging and crack branching was also presumed to be the other mechanisms that contributed to the toughening effects of the composites. In the meantime microcracking and similarly stated by king et al. [39] is an alternative toughening effect in the composites of $TiB_2$-SiC composites. Extra fracture energy is used up in this mechanism via microcracking due to the interfacial stress made at the SiC/$TiB_2$ grain boundaries. This mechanism is initiated by the lack of congruence between the coefficient of heat expansion of the SiC grains and $TiB_2$. Therefore, a shield is created by microcracking at the tip of a propagating crack, which consequently improves toughness [43]. In summary, the alteration of the fracture mode from intergranular to mainly transgranular approach is initiated by the introduction of SiC as revealed from the fractured surface (Fig. 10), hence the crack movement energy is caused by the combination of the toughening mechanism during the fracturing process tends to improve the fracture toughness.

## 3.5 The influences of Load on Coefficient of Friction (COF) of monolithic $TiB_2$ and doped $TiB_2$ with SiC

The Fig. 13, shows the tribological performance of the sintered materials, it revealed the average COF of the sintered composites, the average COF for the monolithic $TiB_2$ ceramic ranges from 0.16–0.47 with a rise in the load from 5 N to 20 N. The av. COF first increase and then decrease at load 5 N and 10 N respectively as depicted Fig. 13, similarly the same trend was also observed for av. COF of this composite at 15 N and 20 N. The outcomes of monolithic $TiB_2$ demonstrated that lower av. COF (0.16) can be achieved at a higher load of 20 N.

The av. COF of $TiB_2$-10SiC varies in the range of 0.11–0.44 with an increase in the load. The av. COF first increase and then decrease as the load increases. The lower av. COF (0.11) was obtained at a lower and higher load of 10 N and 20 N respectively. The av. COF of $TiB_2$-20SiC varies in the range of 0.11–0.19 with an increase in the load. A recognizable and appreciable lower av. COF was attained for this composite ($TiB_2$-20SiC) at the loads 5 N – 10 N in contrast to monolithic $TiB_2$ and $TiB_2$-10SiC composites.

The COF was observed to be high for the undoped $TiB_2$, however, it got reduced via the increment in the introduction of SiC (Fig. 12). The general decline in the COF for $TiB_2$-20SiC composite was attributed to the creation substantial amount of film by the additive (SiC), which lower the COF of the ceramic composite [44]. Thus this film minimizes the barrier to sliding movement between the contact point of the sample and the load.

# 3.6 The influences of Load on Wear Rates of monolithic $TiB_2$ and doped $TiB_2$ with SiC

The wear rates of monolithic $TiB_2$ and reinforced composites with different percentages of SiC at different loads are depicted in Fig. 14. As the load increased from 5 N to 20 N, the specific wear rates for the monolithic $TiB_2$, ranges from $9.403 \times 10^{-5}$ -$5.149 \times 10^{-4}$ $mm^3$/N.m. The specific wear rate of monolithic $TiB_2$ does not follow a linear pattern, as its specific wear rate first increases at 5 N load and then decreases at 10 N, but at 15 N and 20 N the specific wear rate got increased again. Thus, the least wear rate was achieved at 10 N load. This signifies that at higher load, the undoped $TiB_2$ cannot withstand some higher range of load, this is similarly observed by Zhang et al [45].

For the $TiB_2$-10SiC composites, the specific wear rates increase from $2.866 \times 10^{-5}$-$4.106 \times 10^{-4}$ $mm^3$/N.m as the load increase from 5 N -20 N, while a similar trend was also observed for $TiB_2$-20SiC composites, but its wear rates range from $2.093 \times 10^{-5}$ – $1.5524 \times 10^{-5}$ $mm^3$/N.m. Therefore the least wear rate of $2.866 \times 10^{-5}$ and $2.093 \times 10^{-5}$ was attained for $TiB_2$-10SiC and $TiB_2$-20SiC at 5 N load in contrast to monolithic $TiB_2$ which has a wear rate value of $3.498 \times 10^{-4}$, at a further load of 10 N, 15 N and 20 N, it was examined that the wear rates of the reinforced composites are less than the monolithic $TiB_2$.

The percentage increase in the sintering additive (SiC) influenced the reduction of the wear rate although got increased as the load increases. The wear rate of the monolithic $TiB_2$ was observed to be greater than the composites being reinforced with SiC as depicted in Fig. (13). The composites with a greater percentage of SiC particles depicted the lesser wear rates which were attributed to the solid interfacial bonding between the $TiB_2$ matrix and the SiC reinforcement. More also the optimum hardness and densification of $TiB_2$-20SiC assisted also in the attainment of good wear resistance. More also, the enhancement in the wear resistance can also be credited to the efficient protection of SiC particles on the $TiB_2$ matrix, which limited the fracture and the plastic distortion of the composite [46]. It was further detected that $TiB_2$ and $TiB_2$/SiC (Fig. 15, Fig. 16 and Fig. 17) composites alter with microstructural variation during the sliding wear characteristics. High grains aspect ratio and hard interconnecting linkage of elongated grains initiated improved wear resistance. In addition, intergranular and secondary phases play a significant role in friction and wear performance of $TiB_2$ matrix composites. The individual properties, compositions, etc of these phases are a major contributor to the wear performance of the composites.

# 3.7 Morphological Study of the Worn surface

The worn-out surfaces of the synthesized composites in respect to the applied load are presented in Figs. 15, 16 and 17. Scratches, debris and grooves were seen on the microstructure of the wear tracks. From the micrographs (Fig. 17), a small amount of grooves in the form of scratches is depicted by the

composite with a high percentage of SiC ($TiB_2$-20SiC), hence exhibiting excellent wear resistance. The microstructure of the composite with 10% SiC reinforcement shows some shallow grooves and slight delamination (Fig. 16). Large delamination on the microstructure of the monolithic $TiB_2$ (Fig. 15) was observed, when the load was increased from 15 N to 20 N. The strong adhesion and bond between the sintering additive SiC and the ceramic matrix of $TiB_2$ could be liable for the creation of phases (TiC) that limit the wear of the sample's surface, hence improving the wear resistance. A similar observation by [47] established that the inclusion of particles showed the morphology of minor scratch due to the creation of a strong bond with the matrix alloy. Murthy et al. discovered that the addition of $ZrO_2$ to $B_4C$ ceramic matrix created in-situ $ZrB_2$ which consequently forms round pores of sub-micron size. Hence, the establishment of CO gas could aid to arrest and/or deflect cracks, thus enhancing the tribological behavior of $B_4C$ ceramics.

# 4. The Effects Of Microstructure, Densification And Mechanical Properties On The Wear Performance Of Tib2-sic

The microstructure examination on $TiB_2$-SiC depicted that uniform distribution of the sintering additives was observed to influence the wear behavior of the composites. The discovered in-situ phase especially TiC which was formed had a high impact on the enhanced densification and consequently its mechanical properties (hardness, fracture toughness, etc). Conversely, uneven distribution of these additives in the matrix and their mismatch between the matrix and the additives may lead to poor properties of the composites. Studies have been carried out that mechanical features such as fracture toughness, elastic modulus, and hardness have had an immense impact on the wear performance of complicated brittle materials under sliding situations [28, 48, 49].

Concerning the effect of fracture toughness on the wear behavior of materials, the crack bridging and deflection caused by some amount of the sintering additives in the composites is a notable performance that contributes to the developed wear behavior of materials. More also, the resistibility of materials to a localized plastic deformation initiated via either mechanical abrasion or indenter which is a term regarded as hardness also has an impact on the tribology behavior of a material. Thus the little removal of materials or scratches from the surface of a sintered composites during the characterizing of their wear performance can be attributed to the hardness property of the material. The hardness or the solidity of materials is highly dependent on their strength, ductility, strain, elastic stiffness, toughness, plasticity, viscoelasticity, consequently, the deficiency in some of these aforementioned properties in a material may lower its overall hardness property [50]. Significant research has been done to comprehend the impact of component and experimental parameters under sliding conditions on the level of component damage. At the tribo-contact, chemical layer is absent, the sliding wear can be approximately projected via slide across the surface of the brittle components, hence by the creation and spread of lateral cracks, the elimination of the materials happens [28, 51, 52].

# 5. Conclusion

The synthesizing of monolithic $TiB_2$, $TiB_2$-10 %SiC and $TiB_2$-20 %SiC composites were achieved via SPS at 1850 $^oC$ for 10 min under 50 MPa. The following outcomes were discovered:

1. The densification increases as the percentage of the sintering additives increase from 0–20. The composite of $TiB_2$-20 %SiC has the maximum theoretical density of 99.6%

2. One of the in-situ phases especially TiC was discovered to contribute to the enhancement in the mechanical properties

3. The wear performance is hugely linked to the composites which have improved densification, hardness, and fracture toughness. Thus the composites of $TiB_2$-20 %SiC with relative density, hardness, and fracture toughness of 99.5 %, 25.5 GPa and 4.5 $MPa.m^{1/2}$ respectively, depicted the optimum wear resistance in contrast to other composites which has less or no addition of SiC ($TiB_2$, $TiB_2$-10 %SiC). The creation of a substantial amount of film by the additive (SiC) minimized the barrier to sliding movement between the contact point of the sample and the load. Thus the wear rates of the composites were reduced.

# Declarations

- **Ethical Approval**

This review is solely submitted to this journal and has not been published elsewhere. Proper acknowledgement/reference has been accorded to other works.

- **Consent to Participate**

Yes

- **Consent to Publish**

This review is opened for publication

- **Authors Contributions**

This work was achieved in a collaborative effort by all the authors. Mr. S. D OGUNTUYI, PROF. O. T JOHNSON AND Dr. M. B SHONGWE- designed the study performed the experiment, interpreted results and wrote the first draft of the manuscript while Dr. L. TSHABALALA AND DR. N. MALATJI carried out the analysis of the study, managed literature searches and graphical editing. Conclusively, all authors all worked effectively on the proof-reading and the final approval of the manuscript.

- **Funding**

This research was supported by the National Research Foundation of South Africa for the grant, Unique Grant No. 117867.

- **Competing Interests**

N/A

- **Availability of data and materials**

Data and materials are available

# References


1. Bilgi E, Camurlu HE, Akgün B, Topkaya Y, Sevinç N (2008) Formation of TiB2 by volume combustion and mechanochemical process. Mater Res Bull 43:873–881
2. Shahbazi M, Tayebifard SA, Razavi M (2016) Effect of Ni content on the reaction behaviors and microstructure of TiB2-TiC/Ni cermets synthesized by MASHS. Advanced Ceramics Progress 2:22–26
3. Zhang ZH, Shen XB, Wang FC, Lee SK, Wang L (2010) Densification behavior and mechanical properties of the spark plasma sintered monolithic TiB2 ceramics. Materials Science Engineering: A 527:5947–5951
4. Mahaseni ZH, Germi MD, Ahmadi Z, Asl MS (2018) Microstructural investigation of spark plasma sintered TiB2 ceramics with Si3N4 addition. Ceram Int 44:13367–13372
5. Zheng L, Li F, Zhou Y (2012) "Preparation, microstructure, and mechanical properties of TiB 2 using Ti 3 AlC 2 as a sintering aid". J Am Ceram Soc 95:2028–2034
6. Park JH, Koh YH, Kim HE, Hwang CS, Kang ES (1999) Densification and mechanical properties of titanium diboride with silicon nitride as a sintering aid. J Am Ceram Soc 82:3037–3042
7. Ahmadi Z, Nayebi B, Asl MS, Farahbakhsh I, Balak Z (2018) Densification improvement of spark plasma sintered TiB2-based composites with micron-, submicron-and nano-sized SiC particulates. Ceram Int 44:11431–11437
8. Bhaumik SK, Divakar C, Singh AK, Upadhyaya GS (2000) Synthesis and sintering of TiB2 and TiB2–TiC composite under high pressure. Materials Science Engineering: A 279:275–281
9. Shongwe MB, "Spark Plasma Sintering of Ceramic Matrix Composite of TiC: Microstructure, Densification, and Mechanical Properties: A Review" *Advances in Material Science and Engineering: Selected articles from ICMMPE* 2020, p. 93
10. Farhadi K, Namini AS, Asl MS, Mohammadzadeh A, Kakroudi MG (2016) Characterization of hot pressed SiC whisker reinforced TiB2 based composites. International Journal of Refractory Metals Hard Materials 61:84–90
11. Asl MS, Ahmadi Z, Parvizi S, Balak Z, Farahbakhsh I (2017) Contribution of SiC particle size and spark plasma sintering conditions on grain growth and hardness of TiB2 composites. Ceram Int 43:13924–13931

12. Muraoka Y, Yoshinaka M, Hirota K, Yamaguchi O (1996) Hot isostatic pressing of TiB2-ZrO2 (2 mol% Y2O3) composite powders. Mater Res Bull 31:787–792
13. Oguntuyi SD, Johnson OT, Shongwe MB, "Spark Plasma Sintering of Ceramic Matrix Composite of ZrB2 and TiB2: Microstructure, Densification, and Mechanical Properties—A Review" *Metals and Materials International*, 2020/09/27 2020.
14. Oguntuyi SD, Johnson OT, Shongwe MB, "Spark plasma sintering of ceramic matrix composite of TiC: microstructure, densification, and mechanical properties: a review" *The International Journal of Advanced Manufacturing Technology*, pp. 1–14, 2021
15. Jiang D, Van der Biest O, Vleugels J (2007) "ZrO2–WC nanocomposites with superior properties". J Eur Ceram Soc 27:1247–1251
16. Oguntuyi SD, Johnson OT, Shongwe MB, "Spark Plasma Sintering of Ceramic Matrix Composite of ZrB 2 and TiB 2: Microstructure, Densification, and Mechanical Properties—A Review" *Metals and Materials International*, pp. 1–14, 2020
17. Balak Z, Zakeri M, Rahimipoor MR, Salahi E, Azizieh M, Kafashan H (2016) Investigation of effective parameters on densification of ZrB2-SiC based composites using taguchi method. Advanced Ceramics Progress 2:7–15
18. Balak Z, Azizieh M (2018) Oxidation of ZrB2-SiC composites at 1600 C: effect of carbides, borides, silicides, and chopped carbon fiber. Advanced Ceramics Progress 4:18–23
19. Oguntuyi SD, Johnson OT, Shongwe MB, Jeje SO, Rominiyi AL, "The effects of sintering additives on the ceramic matrix composite of ZrO2: microstructure, densification, and mechanical properties–a review" *Advances in Applied Ceramics*, pp. 1–17, 2021
20. Zhang W, Yamashita S, Kita H (2020) "Progress in tribological research of SiC ceramics in unlubricated sliding-A review. Materials Design 190:108528
21. Namini AS, Gogani SNS, Asl MS, Farhadi K, Kakroudi MG, Mohammadzadeh A (2015) Microstructural development and mechanical properties of hot pressed SiC reinforced TiB2 based composite. International Journal of Refractory Metals Hard Materials 51:169–179
22. Asl MS, Namini AS, Kakroudi MG (2016) Influence of silicon carbide addition on the microstructural development of hot pressed zirconium and titanium diborides. Ceram Int 42:5375–5381
23. Asl MS, Delbari SA, Shayesteh F, Ahmadi Z, Motallebzadeh A (2019) Reactive spark plasma sintering of TiB2–SiC–TiN novel composite. International Journal of Refractory Metals Hard Materials 81:119–126
24. Ahmadi Z, Hamidzadeh Mahaseni Z, Dashti Germi M, Shahedi Asl M (2019) Microstructure of spark plasma sintered TiB2 and TiB2–AlN ceramics. Advanced Ceramics Progress 5:36–40
25. Kim HJ, Choi HJ, Lee JG (2002) Mechanochemical synthesis and pressureless sintering of TiB2–AlN composites. J Am Ceram Soc 85:1022–1024
26. Shayesteh F, Delbari SA, Ahmadi Z, Shokouhimehr M, Asl MS (2019) Influence of TiN dopant on microstructure of TiB2 ceramic sintered by spark plasma. Ceram Int 45:5306–5311

27. Alexander R, Ravikanth KV, Bedse RD, Murthy TSRC, Dasgupta K (2019) Effect of carbon fiber on the tribo-mechanical properties of boron carbide: Comparison with carbon nanotube reinforcement. International Journal of Refractory Metals Hard Materials 85:105055
28. Sharma SK, Kumar BVM, Kim Y-W (2015) Effect of WC addition on sliding wear behavior of SiC ceramics. Ceram Int 41:3427–3437
29. Sonber JK, Limaye PK, Murthy TSRC, Sairam K, Nagaraj A, Soni NL et al (2015) "Tribological properties of boron carbide in sliding against WC ball". International Journal of Refractory Metals Hard Materials 51:110–117
30. Fukuhara M, Fukazawa K, Fukawa A, "Physical properties and cutting performance of silicon nitride ceramic," *Wear*, vol. 102, pp. 195–210, 1985
31. Anstis GR, Chantikul P, Lawn BR, Marshall DB (1981) "A critical evaluation of indentation techniques for measuring fracture toughness: I, direct crack measurements". J Am Ceram Soc 64:533–538
32. Evans AG, Charles EA (1976) Fracture toughness determinations by indentation. Journal of the American Ceramic society 59:371–372
33. Asl MS (2017) Microstructure, hardness and fracture toughness of spark plasma sintered ZrB2–SiC–Cf composites. Ceram Int 43:15047–15052
34. Farahbakhsh I, Ahmadi Z, Asl MS (2017) "Densification, microstructure and mechanical properties of hot pressed ZrB2–SiC ceramic doped with nano-sized carbon black". Ceram Int 43:8411–8417
35. Asl MS, Farahbakhsh I, Nayebi B (2016) Characteristics of multi-walled carbon nanotube toughened ZrB2–SiC ceramic composite prepared by hot pressing. Ceram Int 42:1950–1958
36. Nguyen V-H, Delbari SA, Namini AS, Ahmadi Z, Van Le Q, Shokouhimehr M et al (2021) "Microstructural evolution of TiB2–SiC composites empowered with Si3N4, BN or TiN: a comparative study". Ceram Int 47:1002–1011
37. Ghafuri F, Ahmadian M, Emadi R, Zakeri M (2019) Effects of SPS parameters on the densification and mechanical properties of TiB2-SiC composite. Ceram Int 45:10550–10557
38. Asl MS, Kakroudi MG, Rezvani M, Golestani-Fard F (2015) Significance of hot pressing parameters on the microstructure and densification behavior of zirconium diboride. International Journal of Refractory Metals Hard Materials 50:140–145
39. King DS, Fahrenholtz WG, Hilmas GE (2013) "Microstructural Effects on the Mechanical Properties of SiC-15 vol% TiB 2 Particulate-Reinforced Ceramic Composites". J Am Ceram Soc 96:577–583
40. Lin J, Yang Y, Zhang H, Gong J (2017) Effects of CNTs content on the microstructure and mechanical properties of spark plasma sintered TiB2-SiC ceramics. Ceram Int 43:1284–1289
41. Chen H, Wang Z, Wu Z (2014) "Investigation and characterization of densification, processing and mechanical properties of TiB2–SiC ceramics. Materials Design 64:9–14
42. Momeni MM, Mirhosseini M, Chavoshi M (2016) Growth and characterization of Ta2O5 nanorod and WTa2O5 nanowire films on the tantalum substrates by a facile one-step hydrothermal method. Ceram Int 42:9133–9138

43. Demirskyi D, Sakka Y, Vasylkiv O (2015) "High-temperature reactive spark plasma consolidation of TiB2–NbC ceramic composites. Ceram Int 41:10828–10834
44. Aizawa T, Akhadejdamrong T, Mitsuo A (2004) Self-lubrication of nitride ceramic coating by the chlorine ion implantation. Surface Coatings Technology 177:573–581
45. Zhang W, Yamashita S, Kita H (2020) Effects of load on tribological properties of B4C and B4C-SiC ceramics sliding against SiC balls. J Asian Ceam Soc 8:586–596
46. Kaviti RVP, Jeyasimman D, Parande G, Gupta M, Narayanasamy R (2018) Investigation on dry sliding wear behavior of Mg/BN nanocomposites. Journal of Magnesium Alloys 6:263–276
47. Raju PVK, Rajesh S, Rao JB, Bhargava N, "Tribological behavior of Al-Cu alloys and innovative Al-Cu metal matrix composite fabricated using stir-casting technique," *Materials Today: Proceedings*, vol. 5, pp. 885–896, 2018
48. Kumar BVM, Kim Y-W, Lim D-S, Seo W-S (2011) Influence of small amount of sintering additives on unlubricated sliding wear properties of SiC ceramics. Ceram Int 37:3599–3608
49. Basu B, Kalin M (2011) Tribology of ceramics and composites: a materials science perspective. John Wiley & Sons
50. LaSalvia JC, Campbell J, Swab JJ, McCauley JW, "Beyond hardness: Ceramics and ceramic-based composites for protection," *Jom*, vol. 62, pp. 16–23, 2010
51. Evans AG, "Wear mechanisms in ceramics" *Fundamentals Friction and Wear of Materials*, 1981
52. Tewari A, Basu B, Bordia RK (2009) Model for fretting wear of brittle ceramics. Acta Mater 57:2080–2087

# Figures

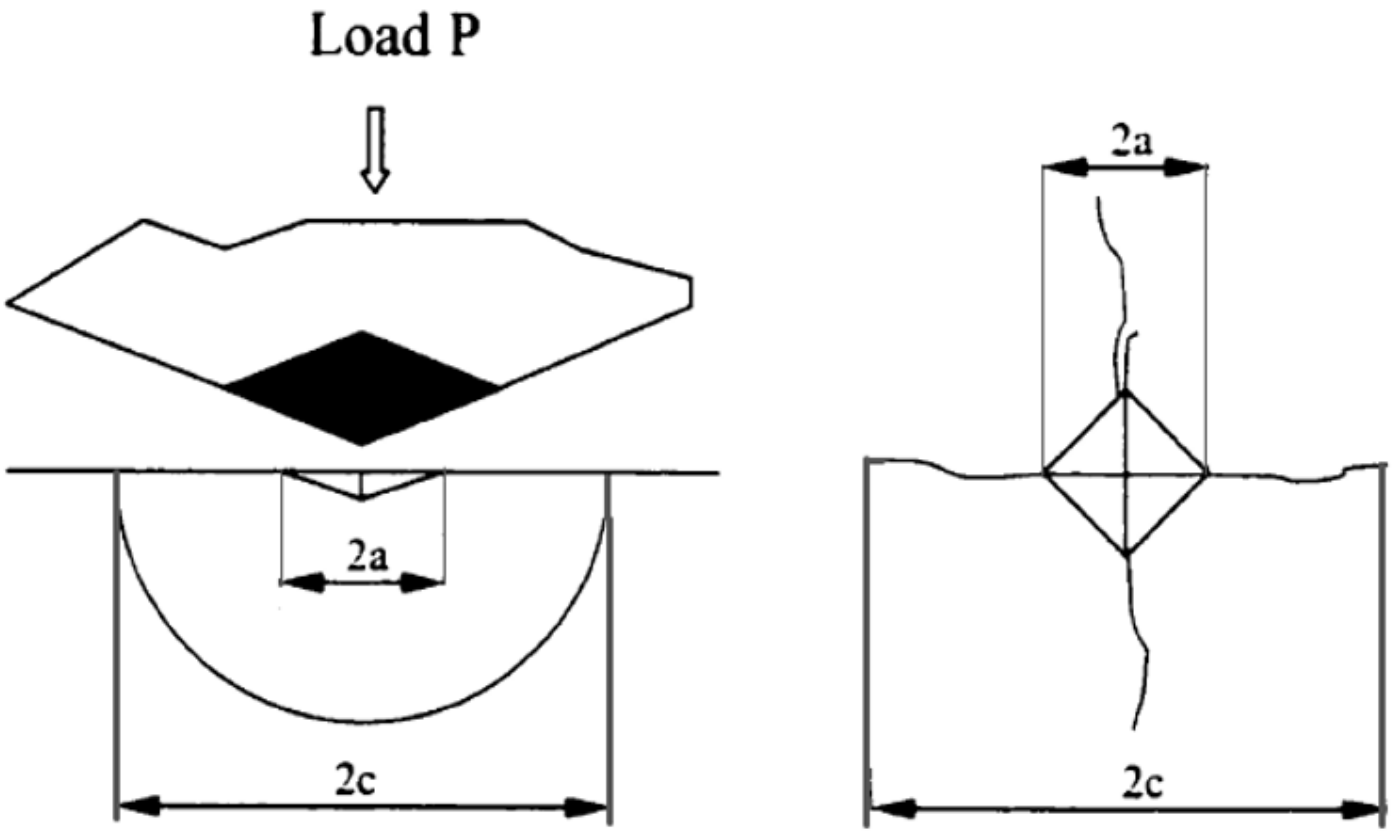


**Figure 1**

Representation for Vickers hardness and indentation test for Fracture Toughness

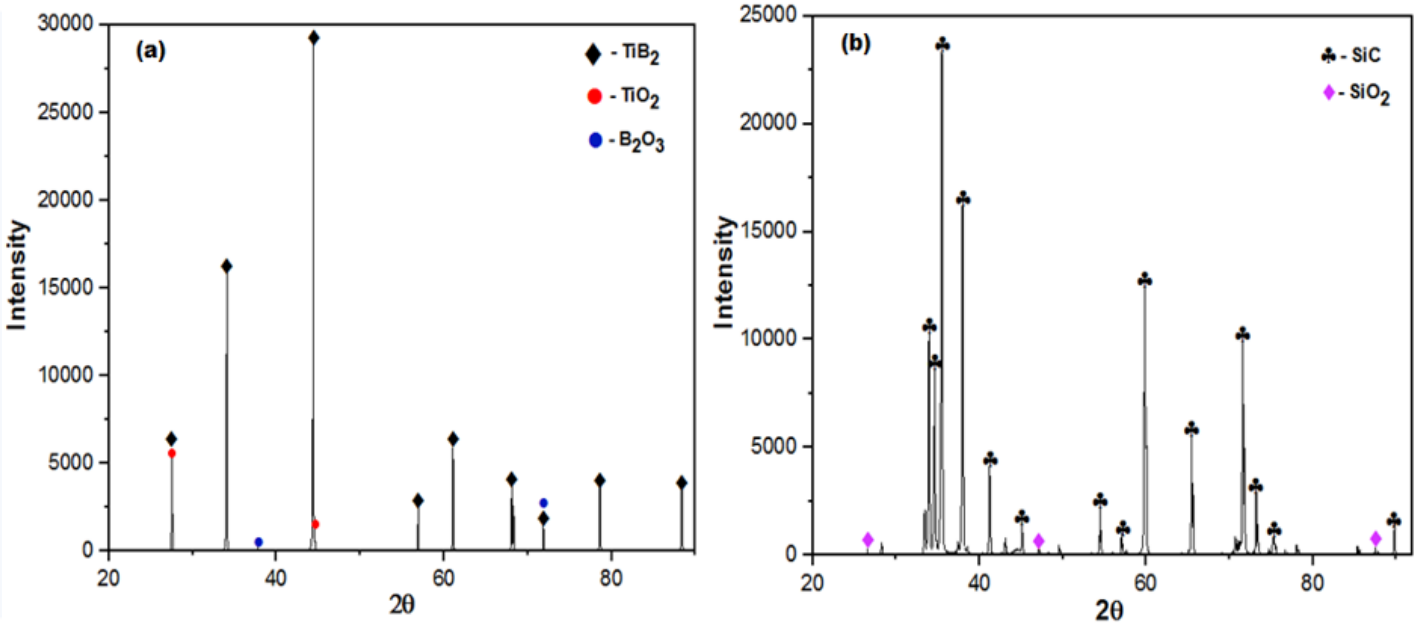


**Figure 2**

XRD of the as-received powder of (a) TiB2, (b) SiC

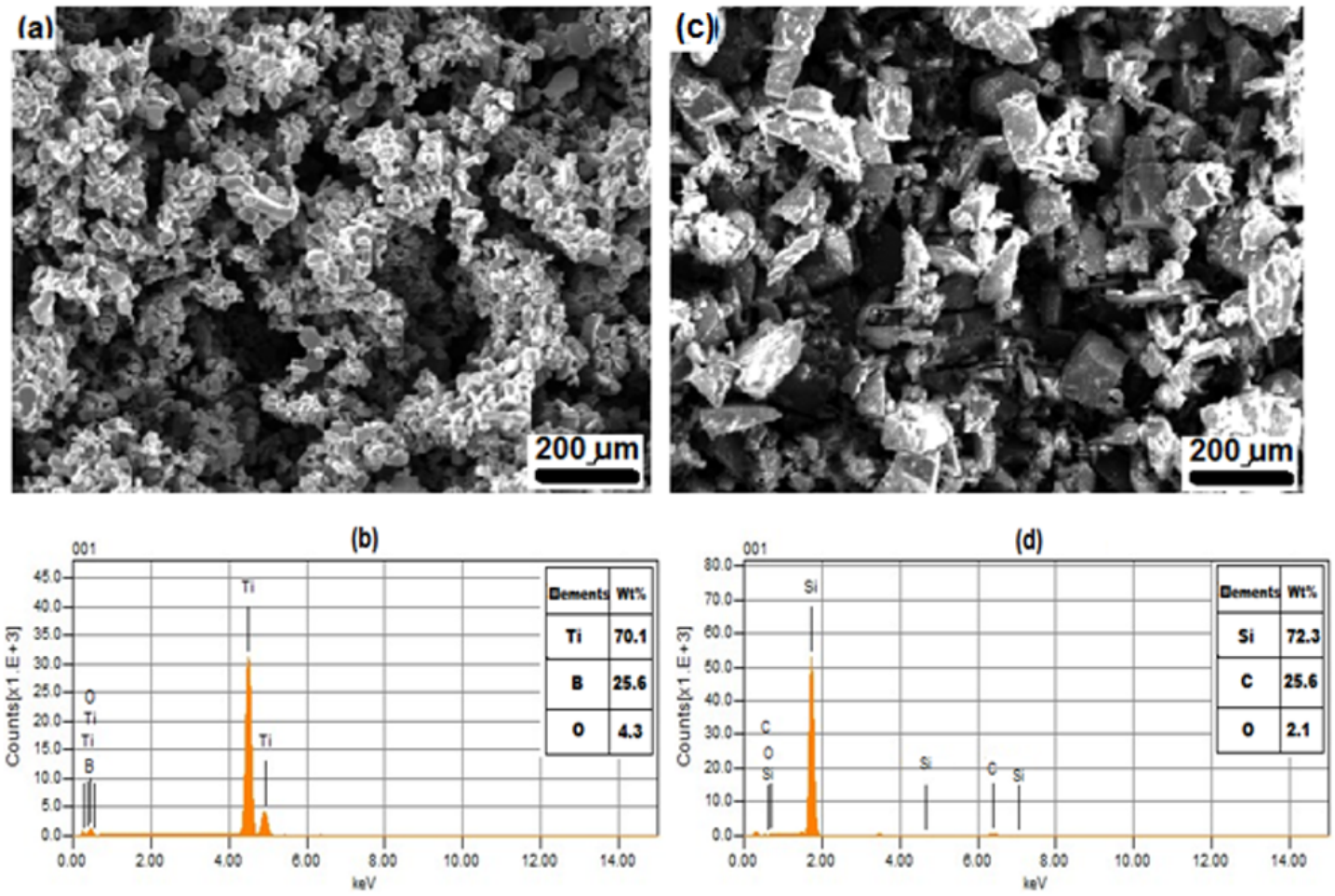


## Figure 3

SEM images and EDX of the as-received powder of TiB2 (a, b) and SiC (c, d)

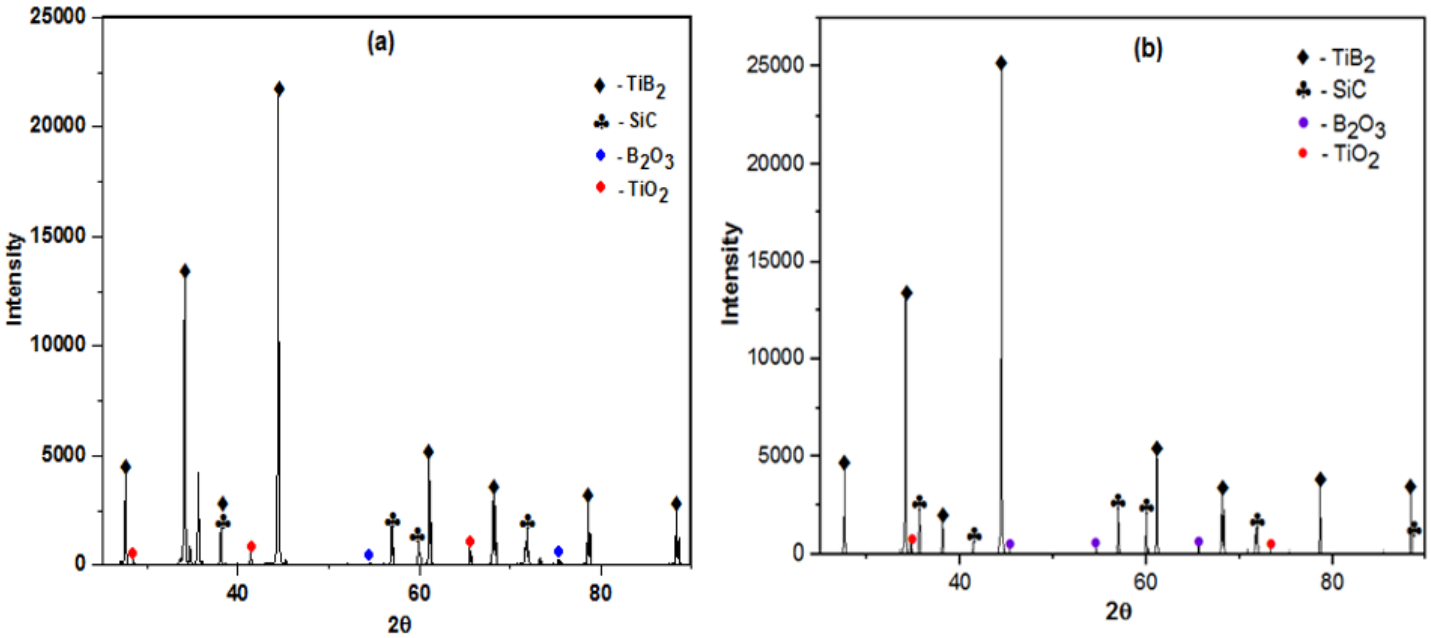

## Figure 4

XRD of mixed composites (a) TiB2-10SiC, (b) TiB2-20SiC

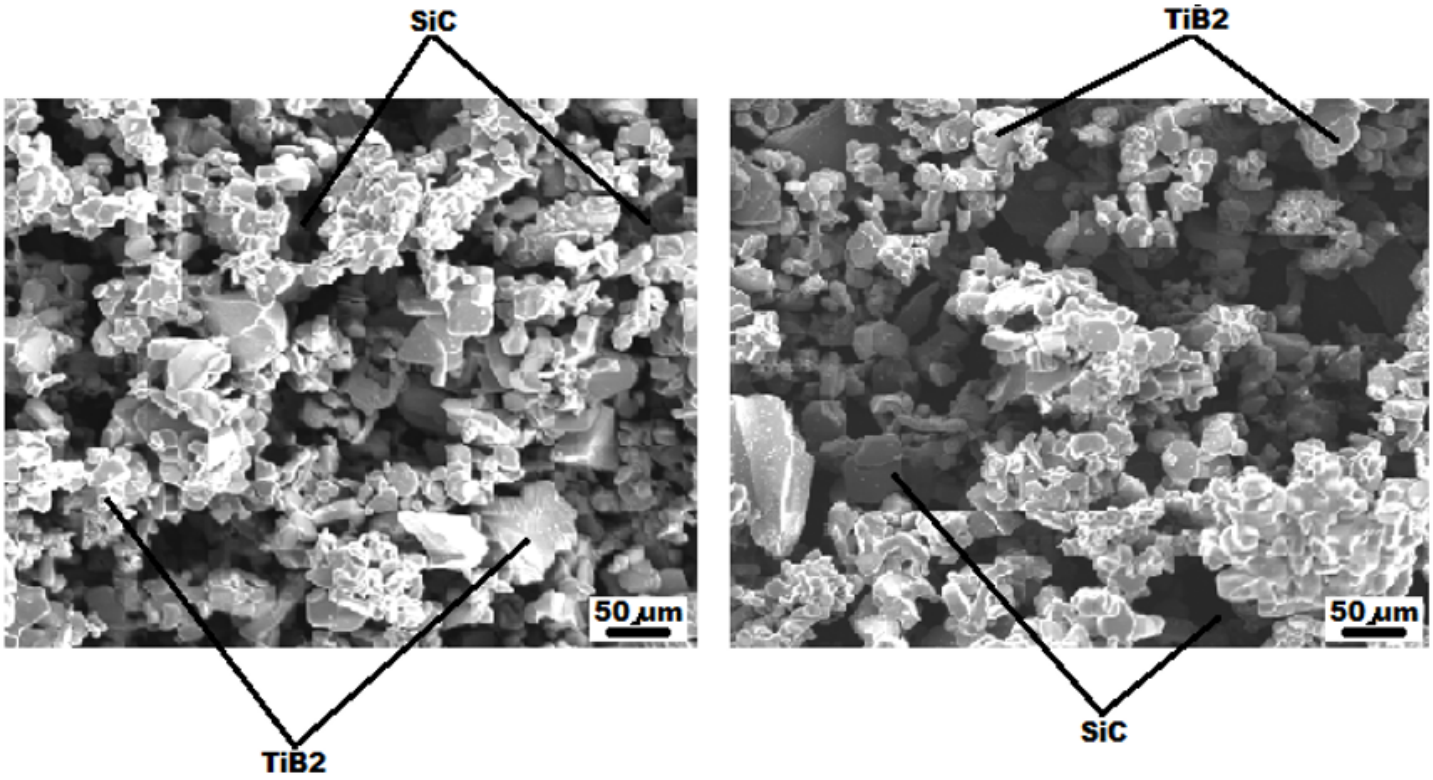


## Figure 5

SEM micrograph of admixed powder (a) TiB2-10SiC, (b) TiB2-20SiC

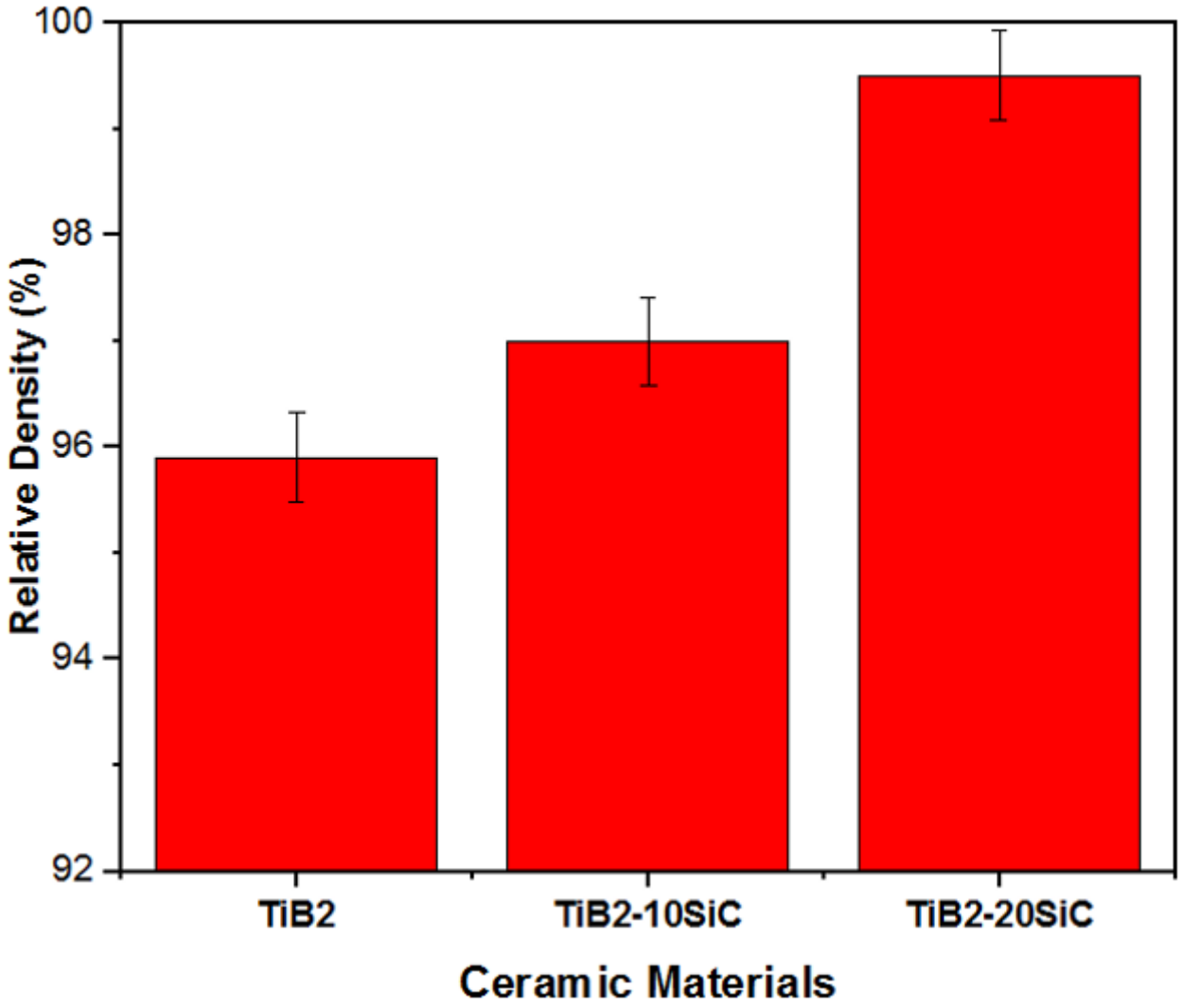


**Figure 6**

Relative density of monolithic TiB2 and doped TiB2-SiC

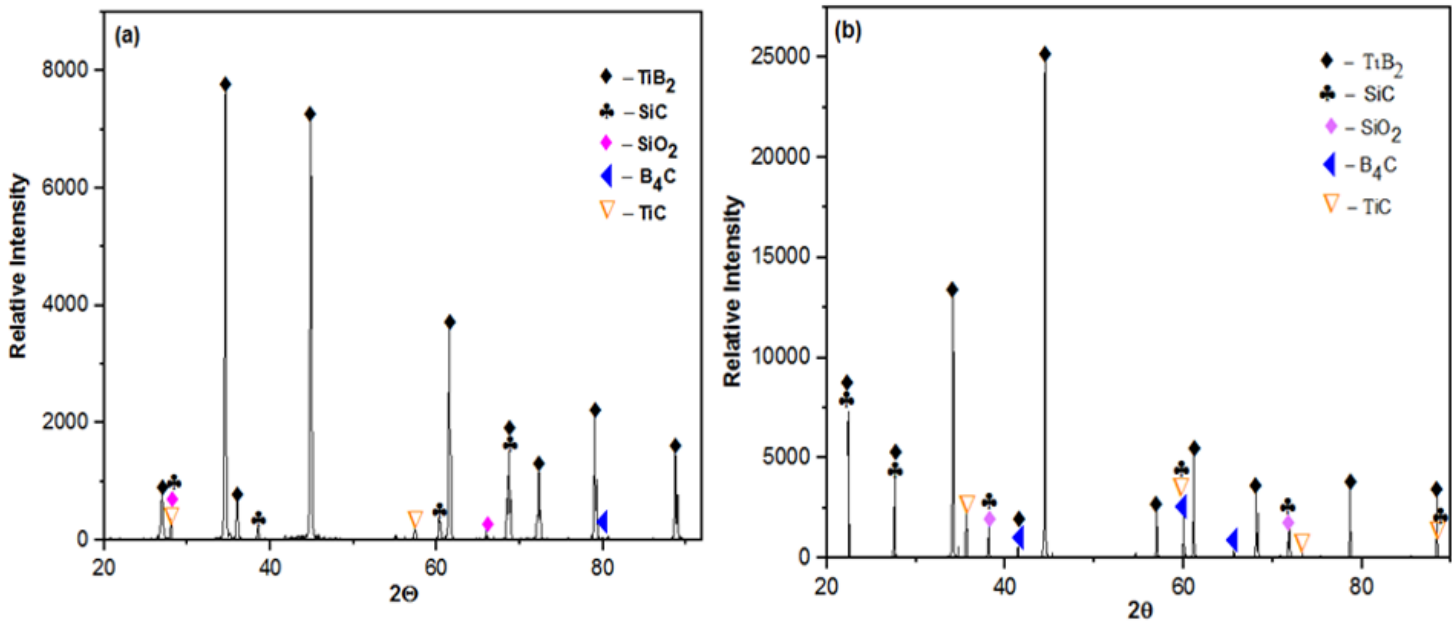

## Figure 7

XRD of as-sintered (a) TiB2-10SiC, (b) TiB2-20SiC

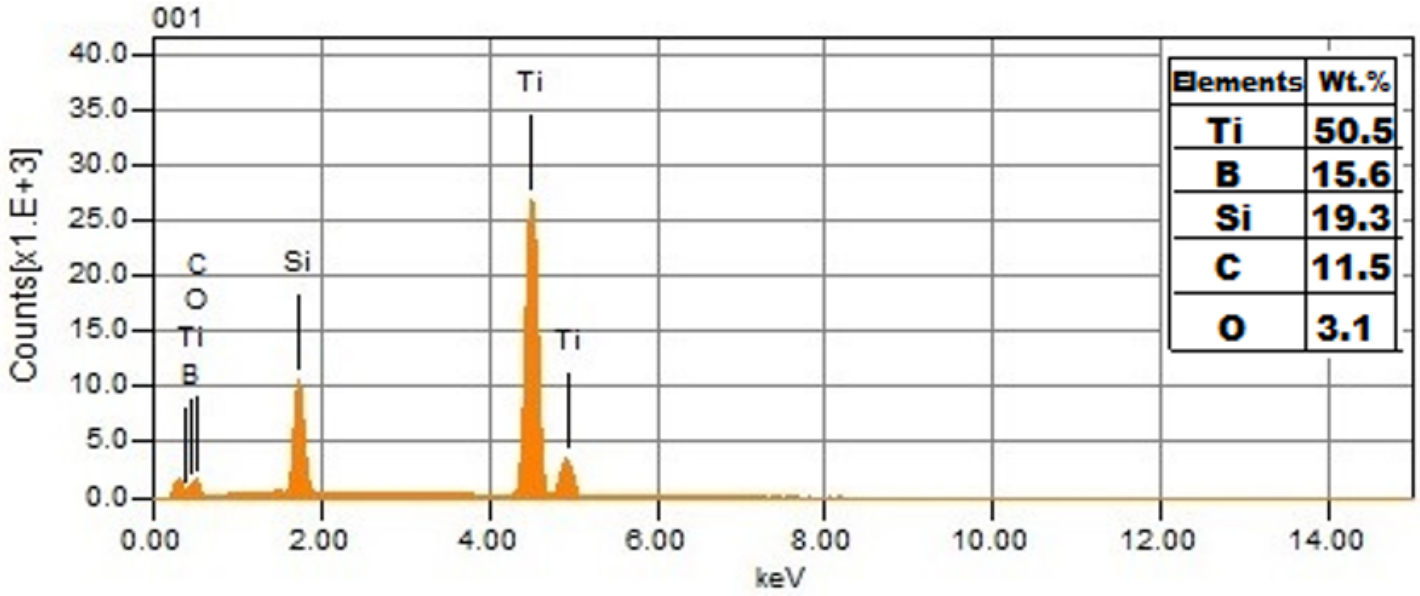


## Figure 8

EDX of sintered TiB2-20SiC

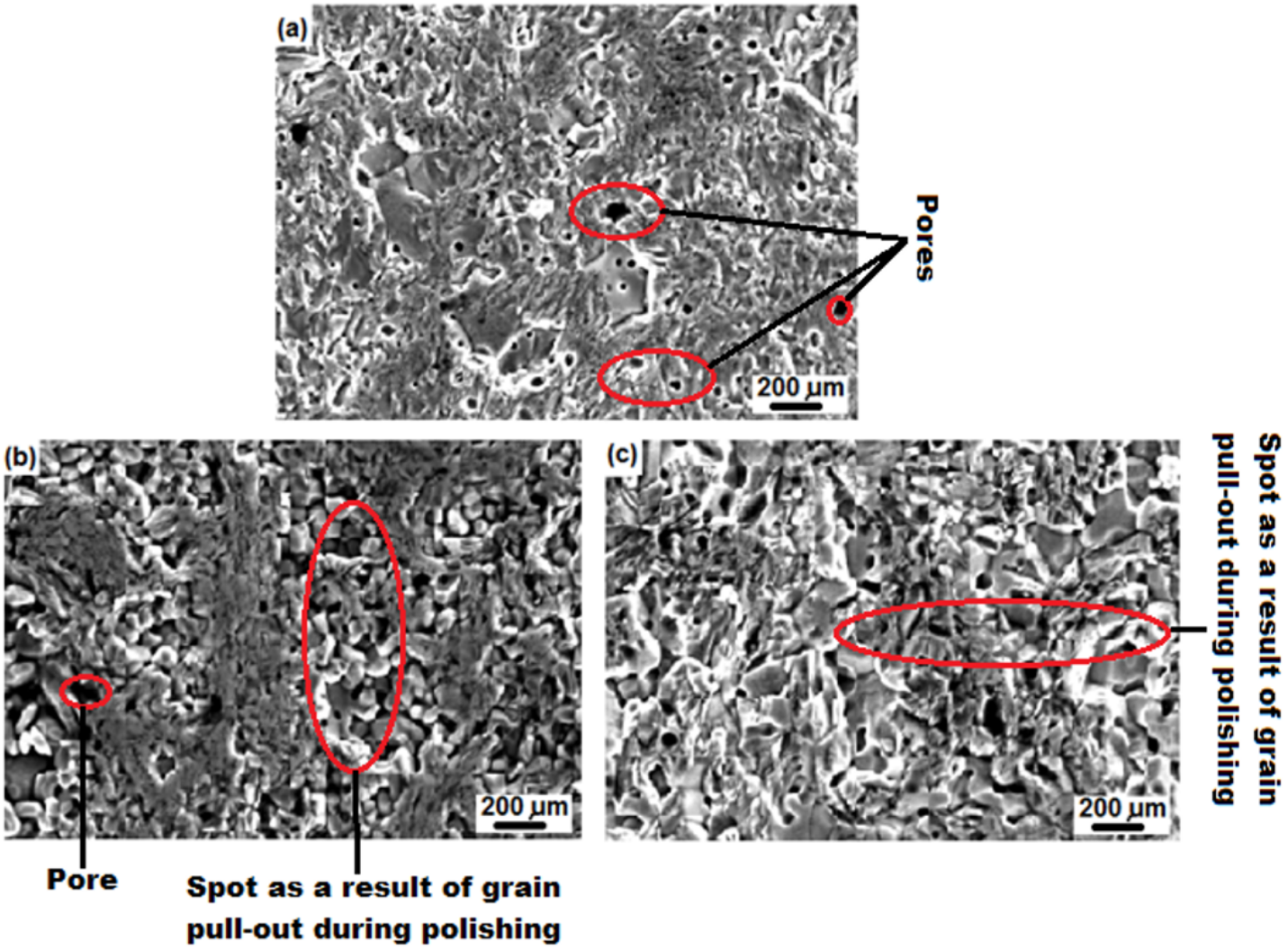


## Figure 9

SEM images of polished sintered (a) monolithic TiB2, (b) TiB2-10SiC (c) TiB2-20SiC

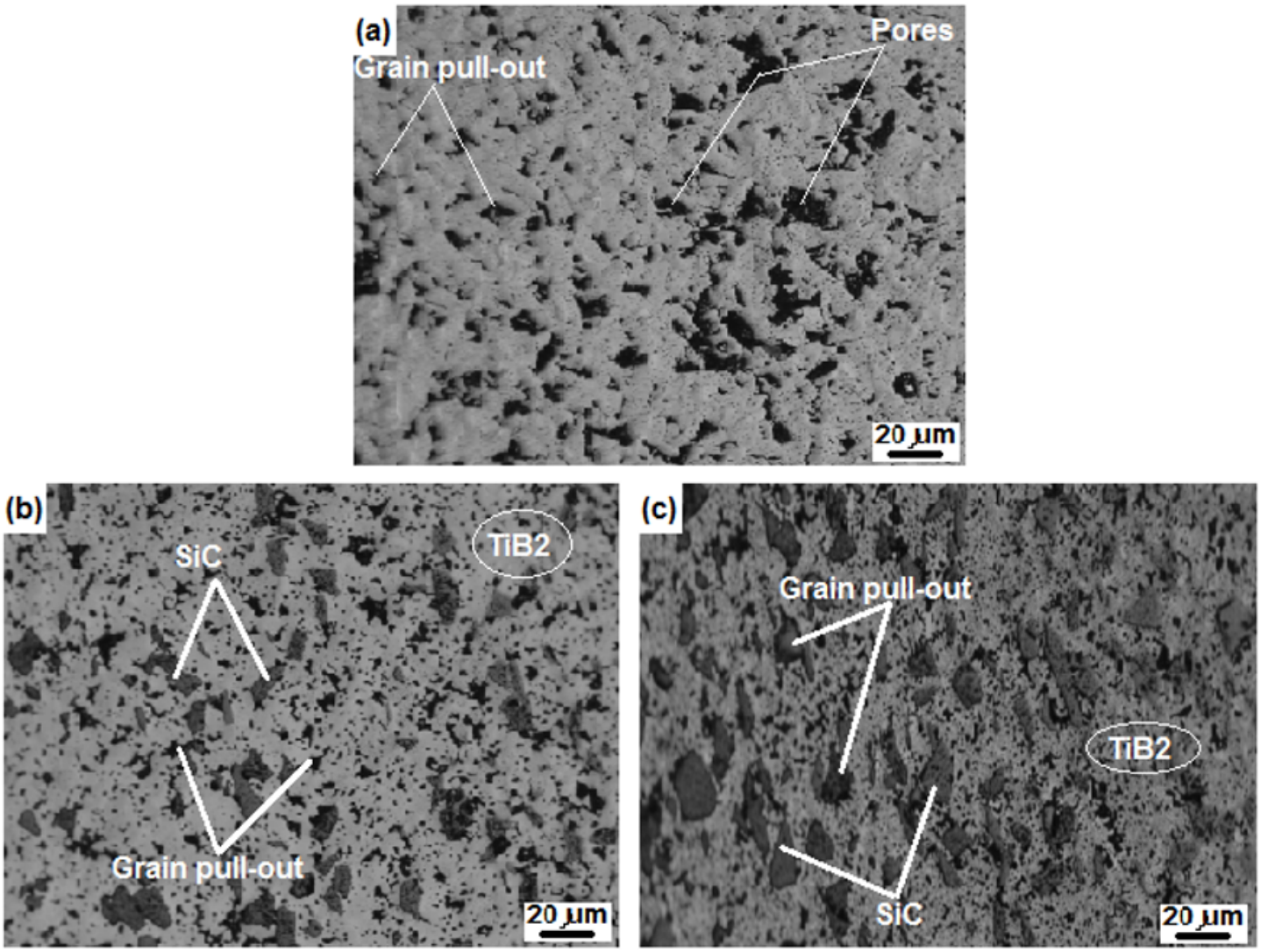


## Figure 10

OPM of polished sintered (a) monolithic TiB2, (b) TiB2-10SiC (c) TiB2-20SiC. The gray phase is the reinforcement of SiC grains. The bright phase is the ceramic matrix grains of TiB2 and lastly, the black phases are pores or some of the pull-out grains during polishing.

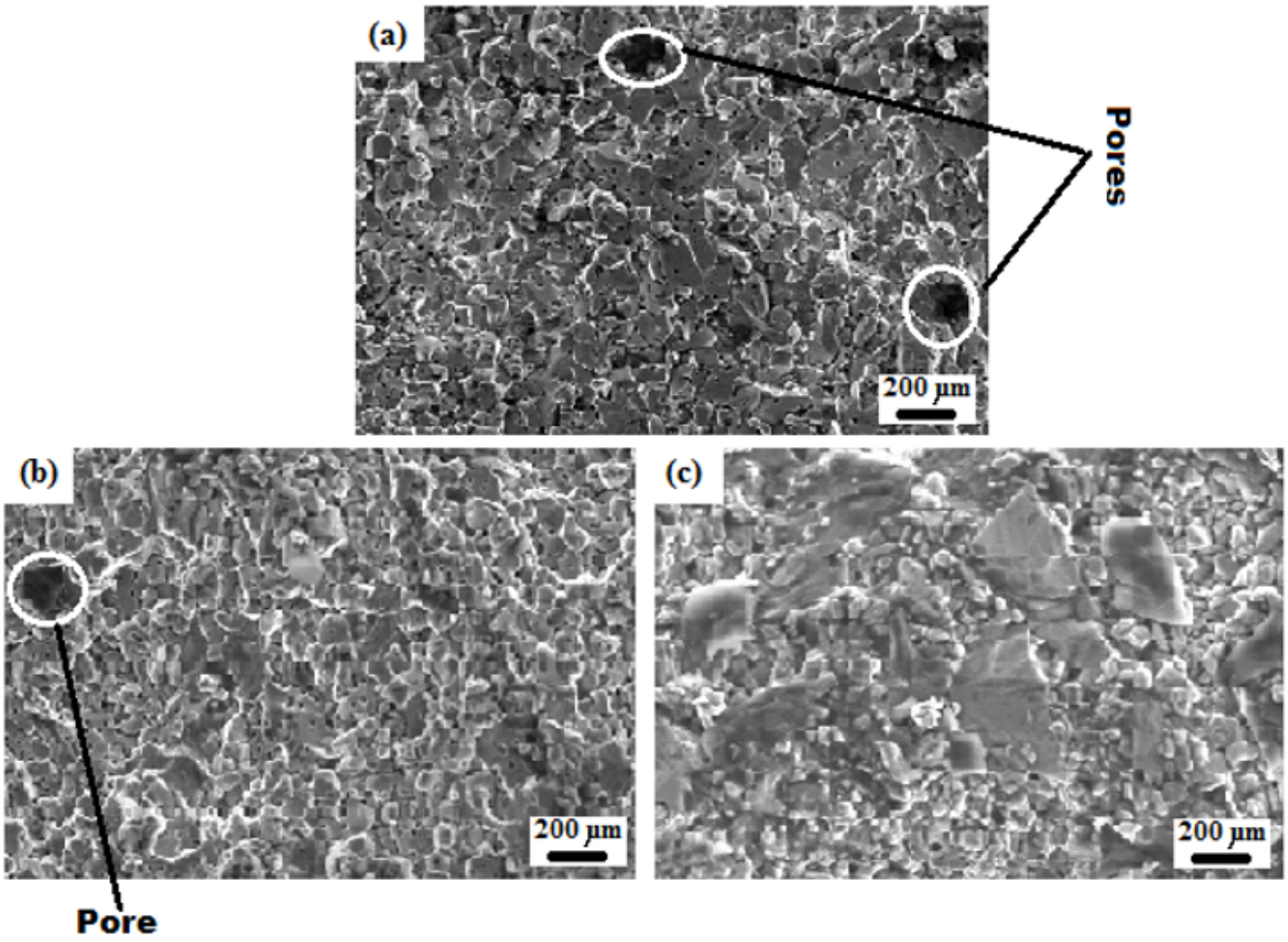


## Figure 11

SEM micrograph of fractured surfaces of (a) monolithic TiB2, (b) TiB2-10SiC (c) TiB2-20SiC sintered at 1850 oC for 10 min under 50 MPa: Showing the pores that are left after being sintered

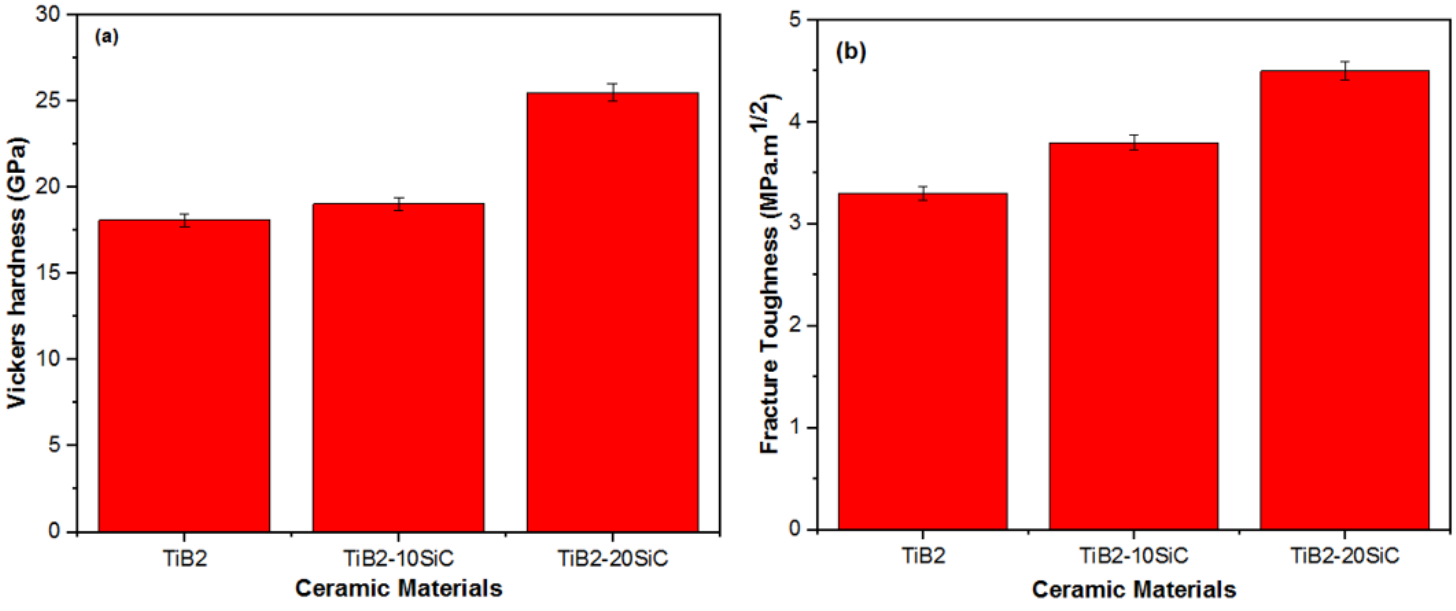

## Figure 12

Mechanical properties of monolithic TiB2 and TiB2 with SiC, (a) Vickers hardness, (b) Fracture toughness

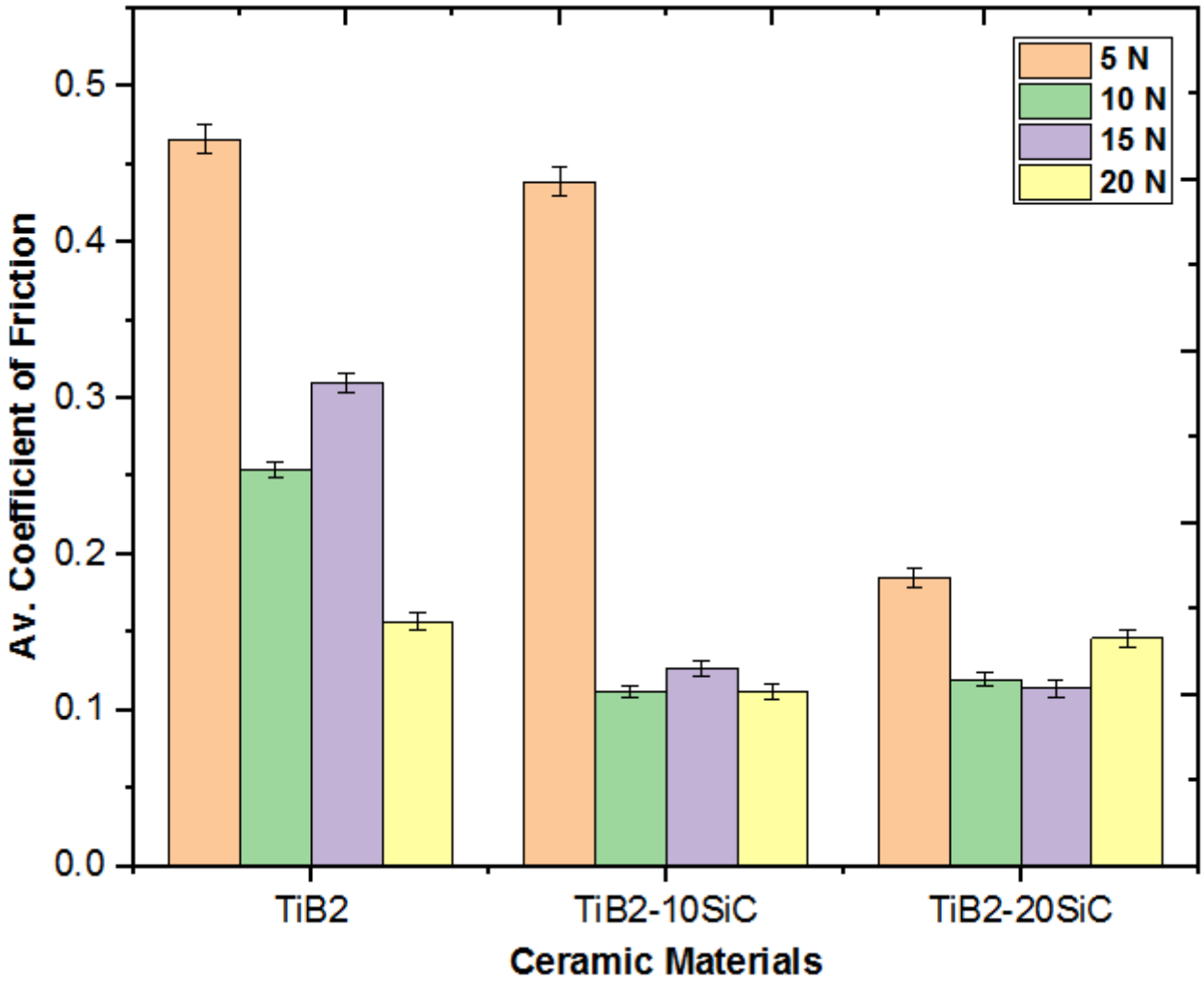


## Figure 13

Average COF of monolithic TiB2 and doped TiB2 with SiC

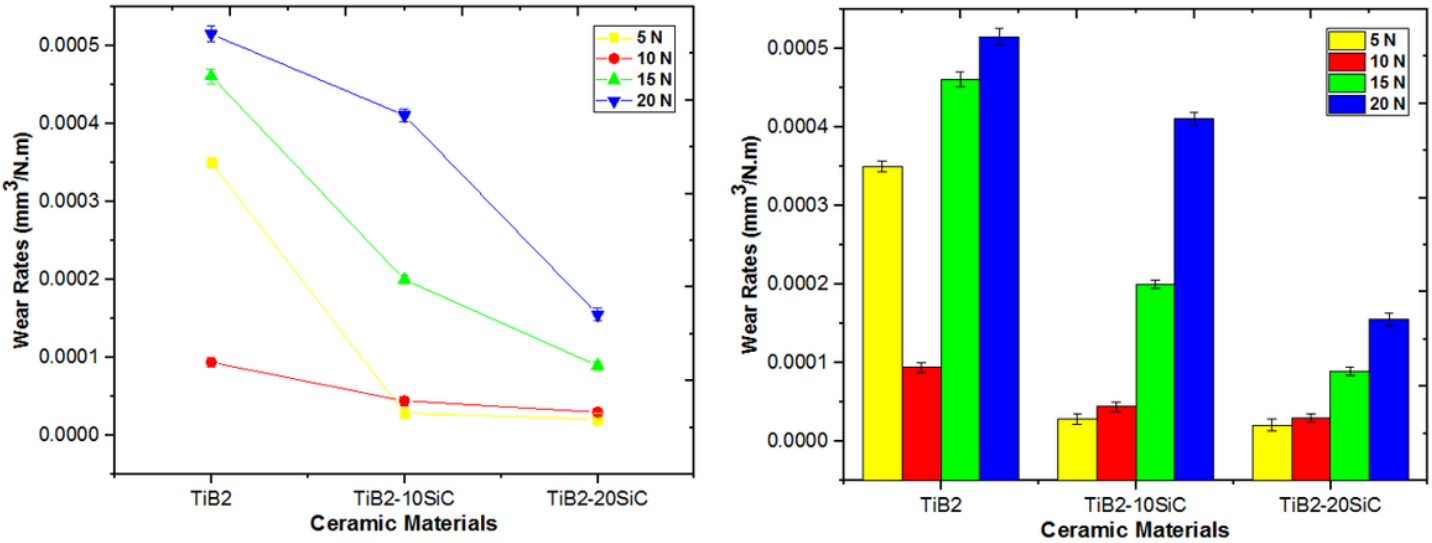

## Figure 14

Wear rates of monolithic TiB2 and doped TiB2 with SiC

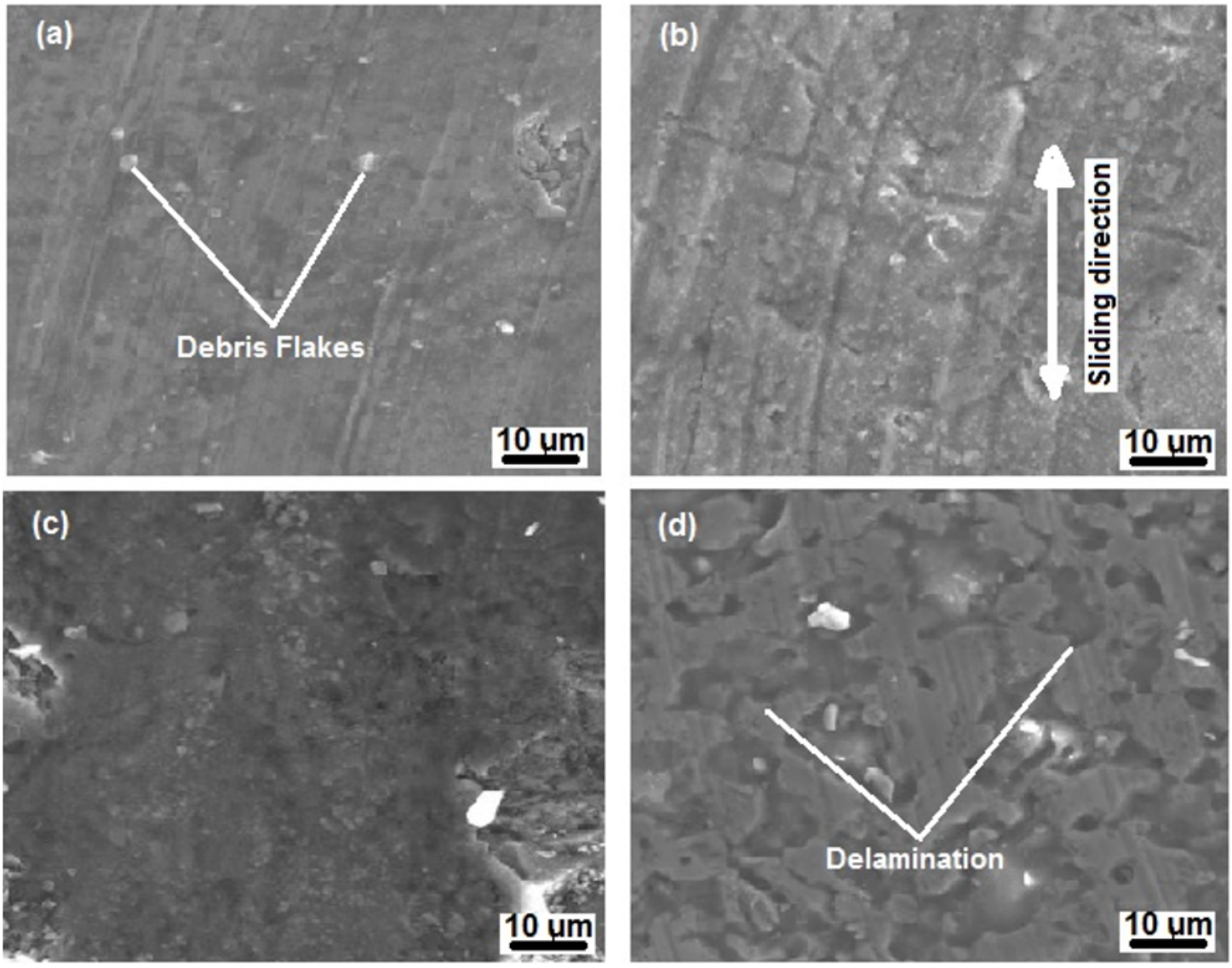


## Figure 15

SEM image of worn-out surfaces of Monolithic TiB2 at a load of (a) 5 N, (b) 10 N, (c) 15 N and (d) 20 N

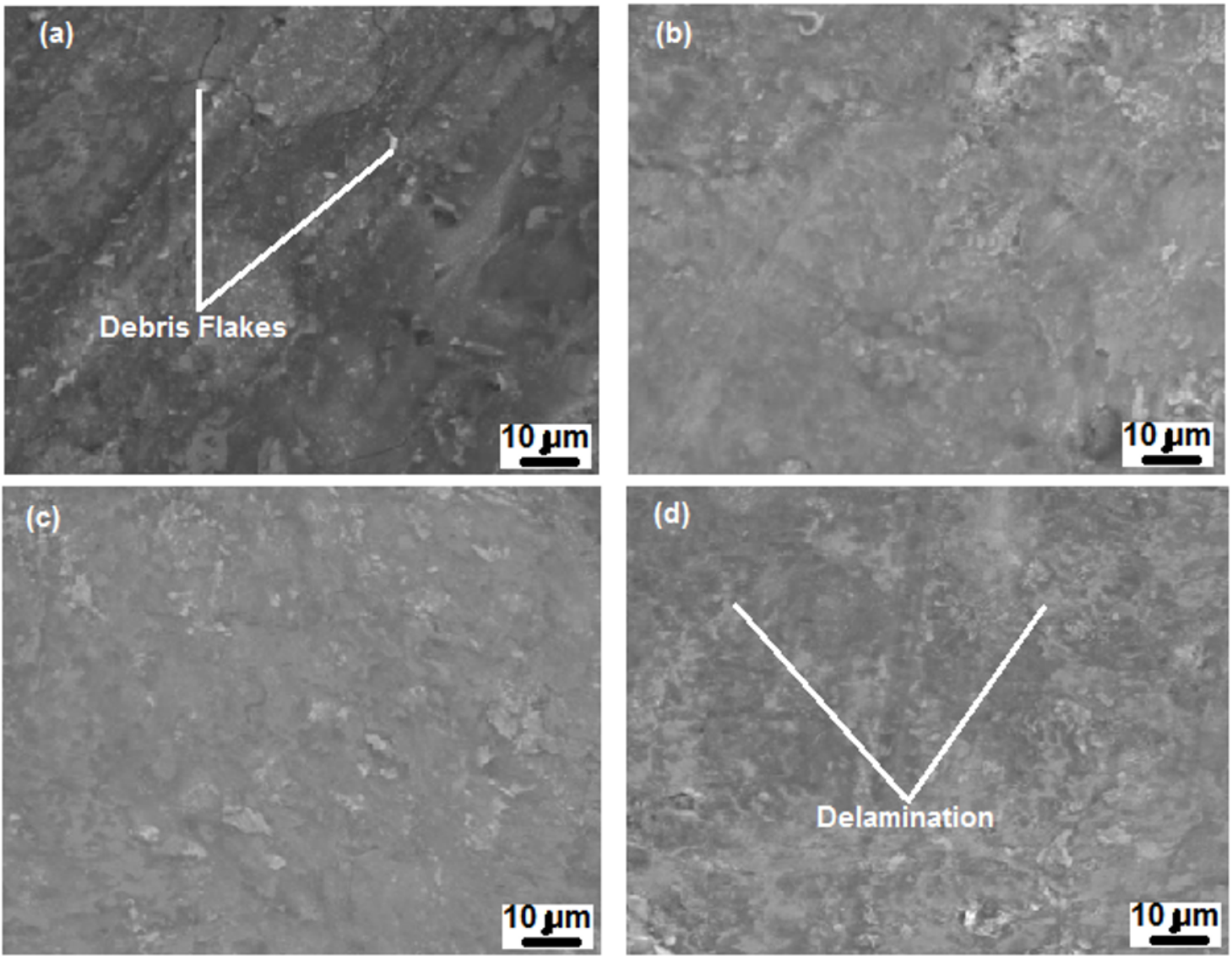


## Figure 16

SEM image of worn-out surfaces of TiB2-10SiC at a load of (a) 5 N, (b) 10 N, (c) 15 N and (d) 20 N

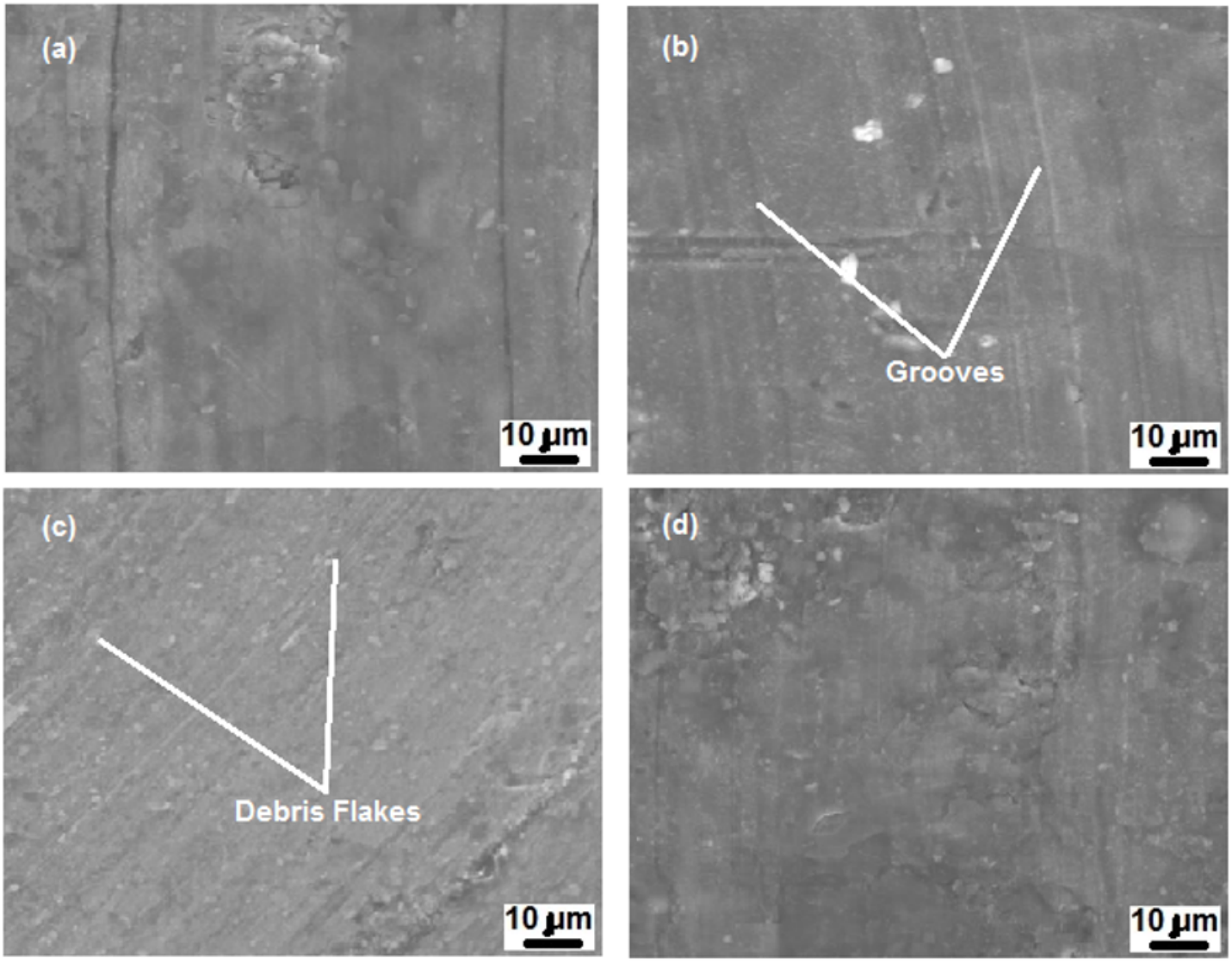


## Figure 17

SEM image of worn-out surfaces of TiB2-20SiC at a load of (a) 5 N, (b) 10 N, (c) 15 N and (d) 20 N